Thermal diversity affects community responses to warming

Bingzhang Chen[a,b]

[a] *Department of Mathematics and Statistics, University of Strathclyde, Glasgow, United Kingdom*
[b] *Hong Kong Branch of Southern Marine Science and Engineering Guangdong Laboratory (Guangzhou), The Hong Kong University of Science and Technology, Clear Water Bay, Hong Kong, China*

Abstract

Scientists often use an exponential equation to model the responses of community metabolic rates to temperature, which however contradicts with the fact that the temperature performance curves of individual species are unimodal, and ignores the difference between intraspecific and interspecific temperature sensitivity. To address these issues, species thermal diversity needs to be considered. To explore how thermal diversity affects community temperature responses, I construct a nutrient-phytoplankton-zooplankton (NPZ) model in which phytoplankton is represented by multiple species with different temperature performance curves. Each curve is determined by a master thermal trait, optimal temperature. I then create two levels of phytoplankton thermal diversity by varying the zooplankton prey density-dependent feeding preference (if zooplankton prefers to feed on abundant prey, prey diversity is enhanced). I find that the responses of the community productivity to temperature is dampened at high diversity compared to low diversity, due to the lower interspecific temperature sensitivity than the intraspecific one. High thermal diversity also confers the community a better capacity to track the environmental temperature fluctuation and withstand high temperature inhibition. In addition, thermal diversity increases community mean optimal temperature. I propose that the community

Email address: bingzhang.chen@strath.ac.uk (Bingzhang Chen)

November 19, 2021

This is a peer reviewed, accepted author manuscript of the following research article:
Chen, B. (2022). Thermal diversity affects community responses to warming. Ecological Modelling, 464, [109846]. https://doi.org/10.1016/j.ecolmodel.2021.109846

temperature sensitivity is not static and urge that distributions of thermal traits of natural assemblages ought to be measured.

Keywords: Activation energy, Phytoplankton, Optimal temperature, Trait variance, Thermal diversity

1. Introduction

How ecosystem productivity responds to climate warming is a central topic in ecology. One key factor is the functional relationship between temperature and the maximal growth or metabolic rate (μ) under resource saturated conditions. For example, Sarmiento et al. (2004) and Taucher and Oschlies (2011) have shown that different choices of functions can lead to opposite predictions of whether ocean primary productivity increases with warming.

Most researchers use a monotonically exponential equation such as the Q_{10} function or the Arrhenius equation to describe the relationship between growth rate and temperature, which is also implemented in the celebrated Metabolic Theory of Ecology and a number of Earth System Models (Eppley, 1972; Brown et al., 2004; Sherman et al., 2016; Kremer et al., 2017; Kwiatkowski et al., 2017). However, a typical temperature performance curve should be unimodal (Montagnes et al., 2003; Angilletta Jr and Angilletta, 2009; Dell et al., 2011; Thomas et al., 2012; Chen, 2015). In other words, growth rate cannot increase infinitely with temperature. This implicates that the usage of a monotonically increasing function might overestimate the growth rates and productivity at high temperatures.

Another relevant issue is the difference between intraspecific (E_a) and interspecific activation energy (E_i) which relates to the thermal adaptation capacity of organisms and the "Hotter-is-better" hypothesis (Huey and Kingsolver, 1989; Knies et al., 2009; Angilletta Jr et al., 2009; Barton and Yvon-Durocher, 2019; Kontopoulos et al., 2020). In the literature of evolutionary biology, the "Hotter-is-better" hypothesis states that the maximal growth rate of each species increases with its optimal temperature and the rate of this increase is similar to

the rate of how growth rate increases with temperature within species. In this paper, I use the notation of E_a to quantify the rate of how growth rate increases with temperature within species, while E_i is the rate of how maximal growth rate increases with optimal temperature across species. One might use E_i to quantify the extent of "hotter is better" and "thermal adaptation". $E_i = 0$ indicates perfect thermal adaptation, while $E_i = E_a$ indicates no adaptation (Barton and Yvon-Durocher, 2019; Kontopoulos et al., 2020). An intermediate value of E_i between zero and E_a indicates partial thermal adaptation (Smith et al., 2019). There are still debates on whether the maximal performances of cold- and warm-adapted species should be equal (i.e., whether E_i should be zero) (Clarke, 2004; Knies et al., 2009; Angilletta Jr et al., 2009). If organisms show some thermal adaptation capacity (e.g., cold-adapted organisms can enhance their metabolic rates relative to the warm-adapted organisms at the same temperature or $E_a > E_i$), it is no longer appropriate to apply a universal monotonic temperature function to describe the temperature response of growth rate.

In this study, I focus on phytoplankton, the dominant primary producers in aquatic ecosystems which account for half of global primary production (Field et al., 1998). It has been observed that phytoplankton E_a is greater than E_i which suggests that the thermal adaptive compensation is significant (Barton and Yvon-Durocher, 2019; Kontopoulos et al., 2020). This suggests that applying a universal temperature function on phytoplankton such as the Eppley curve is problematic.

When one attempts to include multiple species differing in responses to temperature in ecosystem models, an immediate consequence is that the variations of the thermal performance curves, or thermal diversity, will affect the overall temperature response of the community. Intuitively, we would expect that the growth rate of a community consisting of only few species would respond to temperature faster than of a diverse community due to the greater E_a than E_i. However, despite some pioneering studies (Moisan et al., 2002; Burrows et al., 2019), how thermal diversity affects community temperature response has rarely

been investigated.

I aim to investigate the effect of thermal diversity on the community temperature sensitivity quantified as the community-level activation energy (E_w; how fast the community-based growth rate increases with increasing temperature). I first introduce a quantitative framework that builds upon the Metabolic Theory of Ecology and uses optimal temperature as the master thermal trait to model the temperature performance curve which is then parameterized by a phytoplankton laboratory dataset. Then I will simulate how the community-level activation energy varies as a function of the thermal diversity, defined as the variance of optimal temperature, in four environments with different mean temperatures and amplitudes of seasonal temperature fluctuation. I ask the following questions: 1) How will the simulated E_w values differ from the assumed constant value such as 0.32 eV or 0.65 eV (Brown et al., 2004; López-Urrutia et al., 2006; Chen et al., 2012)? 2) How would thermal diversity affect E_w? Does a greater thermal diversity lead to a smaller E_w because it approaches E_i? And whether a smaller thermal diversity leads to a larger E_w that approaches E_a? 3) How will environmental temperature and its fluctuations affect the thermal diversity and subsequent effects on E_w?

2. Materials and methods

2.1. Temperature performance curve

A unimodal temperature performance curve can be expressed as (Johnson and Lewin, 1946; Dell et al., 2011; Chen and Laws, 2017):

$$\mu = \mu_r \frac{e^{\frac{E_a}{k_b}(\frac{1}{T_r}-\frac{1}{T})}}{1+\frac{E_a}{E_h-E_a}e^{\frac{E_h}{k_b}(\frac{1}{T_{opt}}-\frac{1}{T})}} \quad (1)$$

where μ_r is the growth rate at one reference temperature T_r (K). E_h is the nominal activation energy that defines the effect of high temperature inactivation when temperature T exceeds the optimal temperature T_{opt}. k_b is the Boltzmann constant (8.62×10^{-5} eV K^{-1}) (Table 1). If ignoring the part of

Table 1: Annotations and values of the symbols used in this study.

Symbol	Description	Value	Unit
T_r	Reference temperature	288.15	K
k_b	Boltzmann constant	8.62×10^{-5}	eV K^{-1}
T	Environmental temperature		K
x	Transformed environmental temperature	$\frac{1}{k_b}(\frac{1}{T_r} - \frac{1}{T})$	eV^{-1}
T_{opt}	Optimal growth temperature		K
θ	Transformed optimal growth temperature	$\frac{1}{k_b}(\frac{1}{T_r} - \frac{1}{T_{opt}})$	eV^{-1}
σ_θ^2	Variance of θ representing thermal diversity		eV^{-2}
μ_m	Maximal growth rate at T_{opt}	$\mu_0 e^{E_i \theta}$	d^{-1}
μ_0	Normalization constant for μ_m ($\theta = 0$)	0.59	d^{-1}
μ_w	Nutrient-saturated growth rate at the community level	Eq. 7	d^{-1}
E_i	Interspecific activation energy	0.22	eV
E_a	Intraspecific activation energy	$E_{a0} e^{\beta \theta}$	eV
E_{a0}	Normalization constant for E_a ($\theta = 0$)	0.98	eV
β	Scaling exponent against θ for E_a	-0.2	eV
E_h	Nominal activation energy describing how fast μ decreases with T when $x > \theta$	$E_{h0} e^{\phi \theta}$	eV
E_{h0}	Normalization constant for E_h ($\theta = 0$)	4.43	eV
ϕ	Scaling exponent against θ for E_h	0.21	eV
E_w	Activation energy on the community level	Eq. 8	eV
K_N	Half-saturation constant of phytoplankton growth on N	$0.5 e^{E_{Kn} \theta}$	mmol m^{-3}
E_{Kn}	Activation energy of K_N	0, 0.18	eV
α_G	Coefficient of kill-the-winner grazing	1.1, 1.9	dimensionless
M_t	Annual mean environmental temperature	6, 24	°C
A_m	Amplitude of temperature variation	3, 6	°C
K_P	Half-saturation constant of zooplankton grazing	0.5	mmol m^{-3}
I_{m0}	Maximal zooplankton ingestion rate normalized to T_0	1	d^{-1}
m_{z0}	Zooplankton mortality coefficient normalized to T_0	0.15	mmol m^{-3} d^{-1}
γ	Zooplankton gross growth efficiency	0.3	dimensionless

high temperature inhibition, Eq.1 can be simplified to the Arrhenius equation (Brown et al., 2004).

The maximal growth rate (μ_m) at T_{opt} is obtained by substituting $T = T_{opt}$ in Eq. 1:

$$\mu_m = \frac{\mu_r}{1 + \frac{E_a}{E_h - E_a}} e^{\frac{E_a}{k_b}(\frac{1}{T_r} - \frac{1}{T_{opt}})} \tag{2}$$

Substituting Eq. 2 back to Eq. 1 yields:

$$\mu = \mu_m \frac{E_h}{E_h - E_a} \frac{e^{\frac{E_a}{k_b}(\frac{1}{T_{opt}} - \frac{1}{T})}}{1 + \frac{E_a}{E_h - E_a} e^{\frac{E_h}{k_b}(\frac{1}{T_{opt}} - \frac{1}{T})}} \tag{3}$$

For mathematical convenience, I transform T_{opt} and T into θ and x, respectively ($\theta = \frac{1}{k_b}(\frac{1}{T_r} - \frac{1}{T_{opt}})$ and $x = \frac{1}{k_b}(\frac{1}{T_r} - \frac{1}{T})$). As such, Eq. 3 can be converted to:

$$\mu = \mu_m \frac{E_h}{E_h - E_a} \frac{e^{E_a(x-\theta)}}{1 + \frac{E_a}{E_h - E_a} e^{E_h(x-\theta)}} \tag{4}$$

By the definition of E_i,

$$\mu_m = \mu_0 e^{E_i \theta} \tag{5}$$

in which μ_0 is a normalization constant independent of T_{opt}. Similarly, I assume that both E_a and E_h are exponential functions of θ:

$$E_a = E_{a0} e^{\beta\theta} \tag{6a}$$

$$E_h = E_{h0} e^{\phi\theta} \tag{6b}$$

in which E_{a0}, β, E_{h0}, ϕ are all constants independent of θ and will be parameterized by the laboratory data (Table 1).

By substituting Eq. 5 and Eq. 6 back to Eq. 4, we can obtain that θ is the master thermal trait affecting μ, which is the temperature-dependent phytoplankton growth rate under light- and nutrient-replete conditions and is determined by both environmental temperature T and θ.

2.2. Parameter estimation

I use a laboratory dataset of phytoplankton growth rate and temperature merged from Kremer et al. (2017) and Chen and Laws (2017) to estimate the

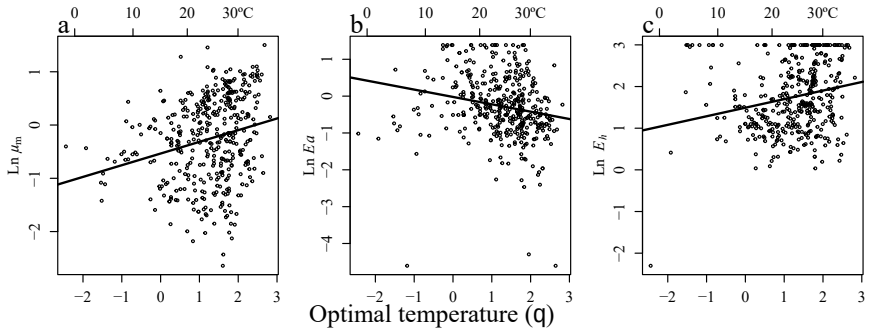

Figure 1: Relationships between log maximal growth rate (μ_m), log activation energies E_a, E_h and transformed optimal temperature (θ). The solid lines represent Ordinary Least-Squares regression lines.

thermal traits (i.e., μ_m, T_{opt}, E_a, and E_h) of each individual taxa following Eq. 4 using the *nls* function in R 4.1.2 (R Core Team, 2021). Then the parameters of μ_0,E_i, E_{a0}, β, E_{h0}, and ϕ are estimated by running Ordinary Least-Square regressions of μ_m, E_a, and E_h against θ following Eq. 5 and Eq. 6 (Fig. 1). As such, a model is obtained to predict μ based on only two inputs, the environmental temperature T and optimal temperature θ.

2.3. Effects of thermal diversity and environmental temperature on community growth rate (μ_w) and activation energy (E_w) under constant temperatures

To illustrate the effect of θ and thermal diversity (σ_θ^2) on community activation energy (E_w), I calculate E_w of three hypothetical communities with different σ_θ^2 values (0.1, 1, 5 eV^{-2}) but the same mean θ along the environmental temperature gradient. While assuming that θ is continuously distributed, I discretize these communities into $M = 41$ species with T_{opt} ranging from -5 to 36 °C. The growth dynamics of all the species follow Eq. 4 and the parameters follow Table 1. The community maximal growth rate (μ_w) is calculated as:

$$\mu_w = \frac{\sum_{i=1}^{M} \mu_i P_i}{P_t} \tag{7}$$

where P_t is the total phytoplankton biomass.

E_w is calculated numerically at each environmental temperature:

$$E_w = \frac{\partial ln(\mu_w)}{\partial x} \tag{8}$$

2.4. *Diversity effects on the temperature sensitivity of phytoplankton under seasonal varying temperatures*

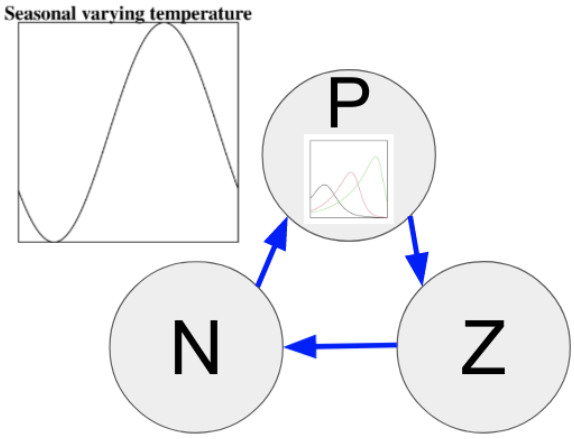

Figure 2: A conceptual diagram of the nutrient-phytoplankton-zooplankton (NPZ) model consisting of multiple phytoplankton species with different T_{opt} driven by seasonal varying temperatures. The blue arrows indicate material flows.

To examine how phytoplankton thermal diversity affects the trait distributions of θ and E_w under seasonal varying temperatures, I run a numerical simulation of a Nitrogen-Phytoplankton-Zooplankton (NPZ) model (Fig. 2) under seasonal variations of temperature at four hypothetical environments. In these cases, σ_θ^2 is no longer an input parameter, but an emergent model output resulting from species interactions in these fluctuating environments.

Environmental temperature (T) is modeled as a cosine function of time (t) (Smith and Amarasekare, 2018):

$$T(t) = M_t - A_m cos\big[\frac{2\pi(t-60)}{365}\big] \tag{9}$$

where M_t is the annual mean temperature. A_m is the amplitude of the variation ($A_m = (T_{max} - T_{min})/2$).

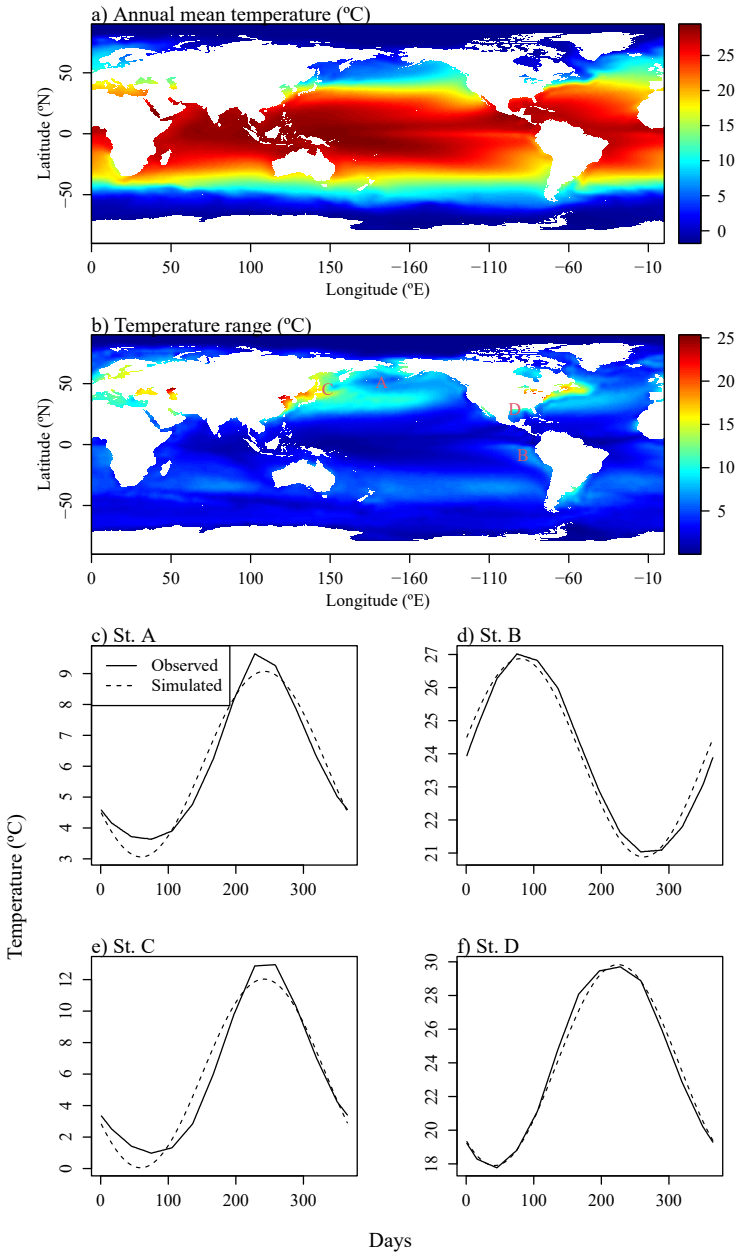

Figure 3: Global distributions of (a) annual mean temperature and (b) temperature range (difference between maximal and minimal temperatures). The red letters indicate the four sites for which the temperature variations are used for simulation. The four panels of (c-f) show the Observed and simulated seasonal variations of sea surface temperatures at the four sites. The annual mean temperatures are 6 °C for St. A & C and 24 °C for St. B & D. The temperature ranges are 6 °C for St. A & B and 12 °C for St. C & D.

To parameterize A_m, I plot the global distributions of M_t and temperature range ($2A_m$) in Fig. 3. The data of daily sea surface temperature were downloaded from `https://www.esrl.noaa.gov/psd/cgi-bin/db_search/DBSearch.pl?Dataset=NOAA+High-resolution+Blended+Analysis&Variable=Sea+Surface+Temperature&group=0&submit=Search` on 22 Dec 2018. A_m values are small in both polar and tropical regions and are largest in temperate waters. Note that Eq. 9 simulates the seasonal variations of temperature well (Fig. 3c-f). I select two values (6 and 24 °C) of M_t to represent the cold and warm environments, respectively. Within each environment, I use two levels of A_m (3 and 6 °C) to generate two levels of temperature variability. These four different temperature environments can be represented by the four sites on Fig. 3b.

The model consists of a single nutrient (dissolved inorganic nitrogen (N), mmol m^{-3}), M phytoplankton species (the same as above), and a single zooplankton compartment (Fig. 2). The nutrient and temperature-dependent growth rate r_i of phytoplankton species i under nutrient concentration N was governed by:

$$r_i = \mu_i \frac{N}{N + K_N} \tag{10}$$

in which K_N is the half-saturation constant for phytoplankton growth on N. The formulation for the maximal growth rate (μ_i) is given by Eq. 4, Eq. 5 and Eq. 6. For simplicity, all phytoplankton species are assumed to share the same K_N which does not vary with T_{opt}. As such, the instantaneous temperature sensitivity of the nutrient-dependent community growth rate is the same with that of the maximal community growth rate under nutrient-replete conditions (E_w). I explored two possible relationships between K_N and environmental temperature: no temperature dependence (the activation energy of K_N (E_{Kn}) is zero) (Smith, 2011; Le Gland et al., 2020) and a positive correlation between K_N and temperature (Aksnes and Egge, 1991; Thingstad and Aksnes, 2019) ($E_{Kn} = 0.18$ eV; Table 1). For the latter case, it is assumed that K_N is the ratio of μ to the affinity α which is determined by physical diffusion of nutrients

towards the cell surface. As the Q_{10} of α is around $1.2 \sim 1.4$ (Thingstad and Aksnes, 2019), the Q_{10} of K_N is roughly $\frac{1.8}{1.4} = 1.3$ which can be converted to an activation energy of 0.18 eV.

The dynamics of phytoplankton species i follow the differential equation below:

$$\frac{\mathrm{d}P_i}{\mathrm{d}t} = r_i P_i - \frac{I_t P_i^{\alpha_G}}{\sum_{i=1}^{M} P_i^{\alpha_G}} \tag{11}$$

where the ingestion of zooplankton (I_t) on total phytoplankton prey is described as:

$$I_t = I_m Z \frac{P_t^2}{P_t^2 + K_P^2} \tag{12}$$

where I_m is the maximal per capita ingestion rate (d^{-1}) and K_P is the half-saturation constant of zooplankton grazing. Z is zooplankton biomass. α_G is the zooplankton kill-the-winner coefficient on phytoplankton. Eq. 11 has the advantage that I_t does not depend on phytoplankton diversity.

Importantly, the diversity difference is generated by varying α_G (Vallina et al., 2014). $\alpha_G = 1$ suggests that there is no frequency-dependent zooplankton grazing while larger α_G values suggests that zooplankton preferentially feed on more abundant species which provides a refuge for rare species and leads to higher diversity. In this study, I use two values of α_G (1.1 vs. 1.9) to generate two treatments with drastically different diversity levels. As such, although phytoplankton thermal diversity changes with seasonally varying temperature at each value of α_G, these changes are much smaller than the difference of thermal diversity induced by different values of α_G.

A constant fraction (i.e., Gross Growth Efficiency (γ)) of zooplankton ingestion is assumed for their reproduction and others are regenerated back to N (Fig. 2). Zooplankton also have a density dependent mortality (Ohman and Hirche, 2001):

$$M_Z = m_z Z^2 \tag{13}$$

Both m_z and I_m have a canonical temperature dependence ($E_Z = 0.65$ eV), conforming to the Metabolic Theory of Ecology (Brown et al., 2004):

$$I_m = I_{m0} e^{E_Z x} \tag{14a}$$

$$m_z = m_{z0} e^{E_Z x} \tag{14b}$$

The dynamics of N follow:

$$\frac{\mathrm{d}N}{\mathrm{d}t} = -\sum_{i=1}^{M} r_i P_i + M_Z + (1-\gamma) I_t \tag{15}$$

Initial concentration of N was set as 1 mmol m^{-3}. The initial biomass for each P_i was set as 0.001 mmol N m^{-3} so that initial P_t was 0.041 mmol N m^{-3}. Initial zooplankton biomass was set as one-tenth of P_t.

I used the Euler forward method to numerically solve the model which was run for 5 years with a time step of 300 seconds. From the second year, the model outputs exhibit regular seasonal cycles. The final year of the output is used for comparisons between different diversity treatments and between different environments. The codes are written in Fortran 90 and are publicly available at `https://github.com/BingzhangChen/Thermal_diversity.git`.

3. Results

3.1. Parameterizing phytoplankton temperature performance curve

I find significant positive trends of μ_m and E_h and a negative trend of E_a with optimal temperature (Fig. 1). The estimated values of μ_0, E_i, E_{a0}, β, E_{h0}, and E_{c2} are shown in Table 1.

An example of the temperature response curves of phytoplankton species with different T_{opt} is shown in Fig. 4a and the fitness (growth rate) landscape on θ at three environmental temperatures is shown in Fig. 4b. The parameterised temperature performance curves of individual species are left skewed (i.e., growth rate declines quickly with increasing temperature when $x > \theta$) (Fig. 4a), which becomes more pronounced when T_{opt} increases. μ_m increases with θ, but at a slower rate than the relationship between μ and x within species because

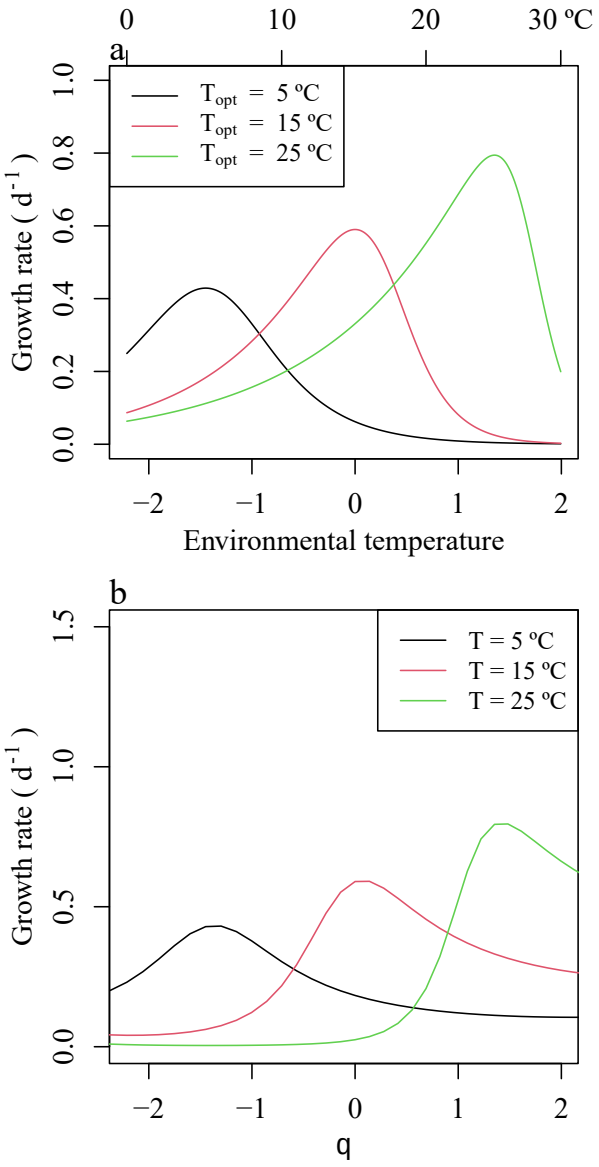

Figure 4: (a) Illustrations of growth rates of three hypothetical phytoplankton species with different T_{opt} along the gradient of environmental temperature. (b) Phytoplankton fitness landscape on transformed optimal temperature θ at three different environmental temperatures (T).

$E_i < E_a$. Under a constant environmental temperature, the fitness landscape is right skewed (i.e., for the same amount of deviation of optimal temperature θ from environmental temperature x (i.e., $|\theta - x|$), warm-adapted species (on the right side of the curve) would perform better than the cold-adapted species (on the left side) (Fig. 4b). This has strong implications on how thermal diversity affects community average optimal temperature as shown below.

3.2. Effects of thermal diversity and environmental temperature on community growth rate and temperature sensitivity under constant temperatures

If environmental temperature and community mean optimal temperature ($\overline{\theta}$) are kept constant, community activation energy (E_w) is affected by both the distance between $\overline{\theta}$ and environmental temperature (i.e, $\overline{\theta} - x$) as well as thermal diversity (σ_θ^2). When the environmental temperature is much lower than $\overline{\theta}$, E_w is close to E_a at both low and intermediate levels of σ_θ^2 (Fig. 5). For the community with the highest σ_θ^2, E_w is lower than other communities because there are more species with optimal temperatures close to the environmental temperature that makes E_w approach E_i. When environmental temperature increases, E_w decreases in all communities. When environmental temperature starts to exceed $\overline{\theta}$, E_w becomes negative. Within physiological temperature ranges (PTR; Pawar et al. (2016)) where $x < \theta$, communities with higher thermal diversity tend to have a lower E_w than those with lower thermal diversity.

In a natural environment, the community properties such as $\overline{\theta}$ and σ_θ^2 are always affected by ever-changing environmental temperature with subsequent effects on E_w. The section below illustrates the dynamics of community $\overline{T_{opt}}$ and σ_θ^2 under realistic seasonal temperature fluctuations.

3.3. Phytoplankton community temperature sensitivity under temperature fluctuation

Unexpectedly, thermal diversity σ_θ^2 affects the dynamics of the community mean optimal temperature $\overline{T_{opt}}$. Here $\overline{T_{opt}}$ has been converted from $\overline{\theta}$ to allow a more intuitive comparison with environmental temperature (Fig. 6). Except for

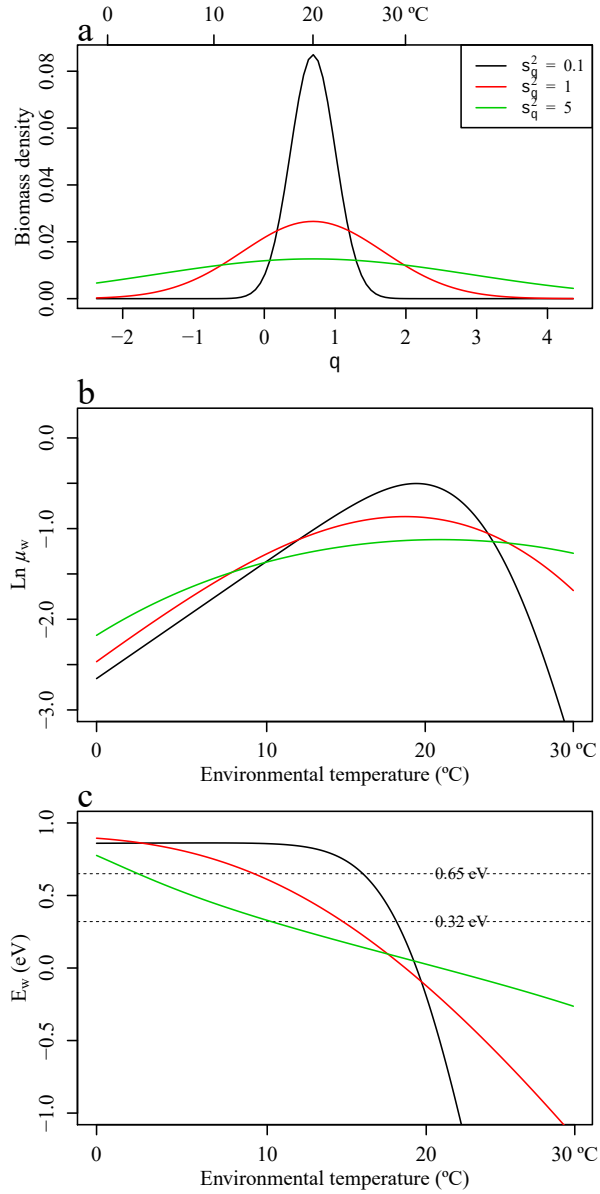

Figure 5: (a) Probability density functions of three hypothetical communities in which θ is normally distributed with different variances (σ_θ^2) but the same $T_{opt} = 20$°C. (b) Log community growth rate (μ_w) of the three hypothetical communities in (a) along the environmental temperature gradient. (c) Community-level activation energy (E_w) of the three communities in (a) along the environmental temperature gradient.

the warm environment with high seasonal temperature variability ($M_t = 24$ °C and $A_m = 6$ °C), $\overline{T_{opt}}$ is always higher in higher diversity treatments ($\alpha_G = 1.9$) than in low diversity treatments ($\alpha_G = 1.1$) (Fig. 6a,e,i). These patterns are not affected by the temperature dependence of K_N which only affects the inorganic nutrient concentration (a smaller K_N in cold environments leads to a lower level of nutrient concentration; compare Fig. 6 with Fig. S3 and Fig. S1 vs. S2).

To explain the increasing trend of $\overline{T_{opt}}$ with σ_θ^2, I compare the biomass distributions of phytoplankton between the two different diversity treatments in Fig. 7. The distributions of T_{opt} appear right skewed with a long tail, which is particularly evident for the high diversity treatment. This is consistent with the fitness (μ_i) landscape along the axis of T_{opt}, which is also right skewed (Fig. 4b). Thus, with increasing σ_θ^2, more species with higher T_{opt} can exist in the community than those with lower T_{opt}, leading to a higher $\overline{T_{opt}}$.

The simulated thermal diversity (σ_θ^2), by design, is always greater in the high diversity than in the low diversity treatment (Fig. 6b,f,j,n). σ_θ^2 is always greater in cold than in warm environments and is greater during the winter than in the summer, reflecting the negative effect of resource competition on diversity (Huston, 1979). While temperature variability does not appreciably affect the magnitude of σ_θ^2, it affects the seasonal variability of σ_θ^2.

Because the responses of $\overline{T_{opt}}$ lag behind environmental temperature (T) in the low diversity treatments, T can exceed $\overline{T_{opt}}$ in later summer particularly in cold and highly fluctuating environments, leading to a negative E_w (Fig. 6). By contrast, in the high diversity treatment, $\overline{T_{opt}}$ tracks T well so that $\overline{T_{opt}}$ are always above T and E_w shows less variability and is often around 0.32 eV.

4. Discussion

I have shown that: i) community temperature sensitivity is unlikely to be a constant value; it is affected by both the local environmental temperature and the distribution of community thermal traits; ii) high thermal diversity reduces the temperature sensitivity of the phytoplankton community but confers the

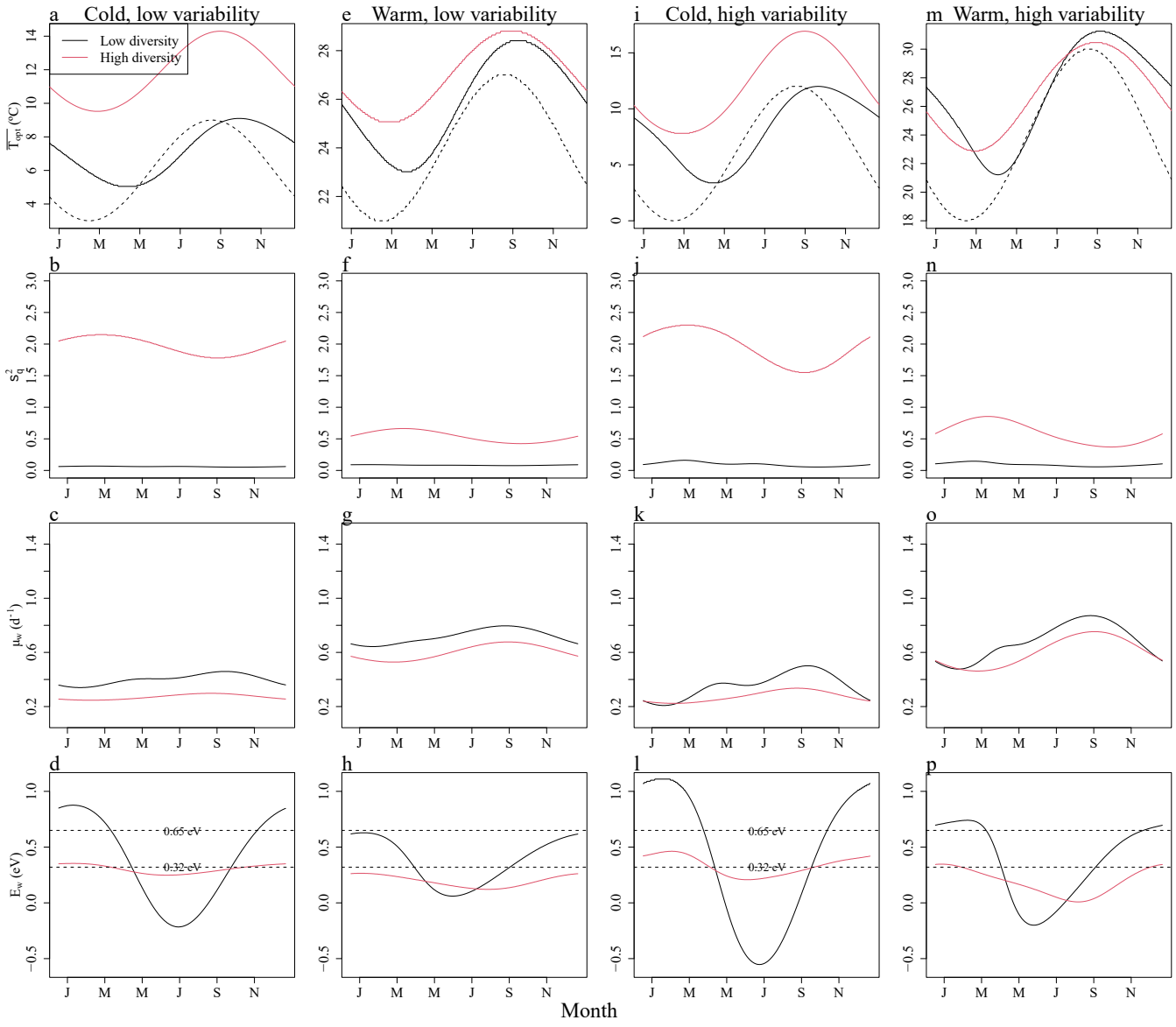

Figure 6: Simulated seasonal patterns of (a, e, i, m) mean T_{opt}, (b,f,j,n) variance of optimal temperature (σ_θ^2), (c, g, k, o) nutrient-saturated growth rate of the phytoplankton community (μ_w), and (d,h,l,p) apparent activation energy on the community level (E_w) in two environments with different temperature variability. The dashed lines in (a, e, i, m) show the seasonal variations of environmental temperature, while those in (d, h, l, p) show the 0.65 and 0.32 eV for comparisons. K_N is independent of temperature in this simulation.

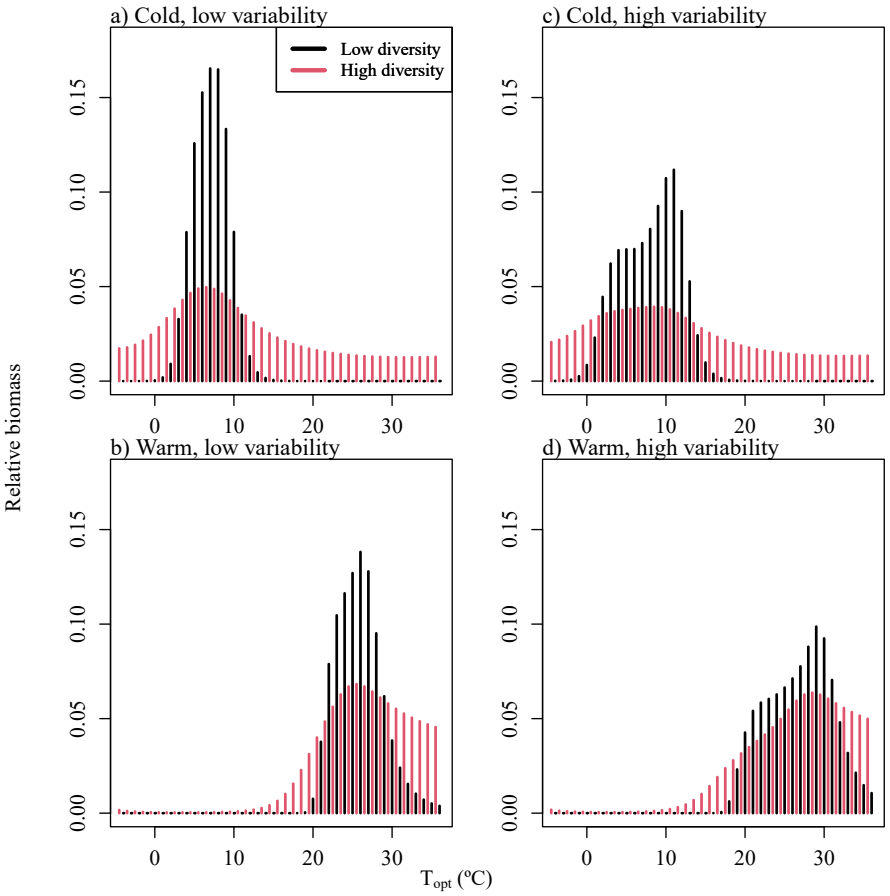

Figure 7: Distributions of the relative biomass of phytoplankton species with different T_{opt} for low and high diversity treatments in (a,c) cold and (b,d) warm environments with different temperature variability.

community a better capacity to withstand high temperature inhibition which is stronger in warm environments; iii) both mean environmental temperature and amplitudes of environmental temperature can affect the effect of thermal diversity on E_w; iv) high thermal diversity leads to a higher optimal temperature due to the asymmetry of the temperature performance curve.

4.1. The community temperature sensitivity is dynamic

My analysis suggests that the community temperature sensitivity E_w is unlikely a static value; it can be affected by the distribution of community T_{opt} relative to the environmental temperature. The temporal variation of E_w is smaller in communities with greater thermal diversity and in colder environments with less temperature variability (Fig. 6).

More specifically, E_w can be affected by the relative distance of mean T_{opt} to the environmental temperature as well as variance and higher-order moments of θ. At the species level, due to the nonlinear nature of the temperature performance curve, when environmental temperature is far below T_{opt}, the apparent activation energy should approach E_a (i.e., not affected by E_h). When environmental temperature approaches T_{opt}, the apparent activation energy should decrease and eventually become negative due to high temperature inhibition. At the community level, E_w is not only affected by the distance between $\overline{T_{opt}}$ and environmental temperature, but also affected by thermal diversity due to the thermal adaptation capacity (i.e., $E_i < E_a$). When the distribution of T_{opt} is flat (i.e., high thermal diversity), E_w should be closer to E_i than E_a and should be less variable than a low diversity community.

In addition, σ_θ^2 can indirectly affect E_w by affecting the mean T_{opt}; a higher σ_θ^2 leads to a higher $\overline{T_{opt}}$. This implies that in regions with greater thermal diversity, the phytoplankton community as a whole will be less vulnerable to high temperature inhibition induced by warming (Huey et al., 2009; Thomas et al., 2012), and vice versa. Thus, to predict how communities will respond to climate warming, we need to have some knowledge of the thermal diversity or distributions of thermal traits of the focal community.

The above analyses and discussions suggest that even in such a simplified and deterministic model system, complex interactions can occur between the environment (i.e., temperature) and organism thermal traits. Given a predefined temperature environment (i.e., given A_m and M_t), E_w can behave in unexpected ways, which is very different from if we use a monotonic function relating growth rate and temperature without high temperature inhibition.

4.2. T_{opt} as a master trait for thermal traits

Trait-based ecology is a powerful framework for understanding community dynamics and relationships between community structure and ecosystem functioning (McGill et al., 2006; Violle et al., 2007). However, one problem with the trait-based approach is that there are often multiple traits corresponding to one single species or individual. Therefore, the dimension of the trait space needs to be reduced (de Bello et al., 2021). Based on Eq. 4, the relevant traits can include μ_m, E_a, and E_h. While I do not deny the effects of other traits on affecting temperature sensitivity, the usage of T_{opt} as the primordial thermal trait has the advantage that 1) it is straightforward to understand and relatively easy to measure; 2) it has been found that other traits are correlated with T_{opt}; 3) there has been a plentiful literature (Norberg, 2004; Thomas et al., 2012; Chen, 2015; Boersma et al., 2016; Burrows et al., 2019) on T_{opt} that can guide future study.

Other environmental factors like light or nutrient limitation can also affect T_{opt} (Edwards et al., 2016; Thomas et al., 2017; Bestion et al., 2018). This can be further incorporated into Eq. 4 by adding additional effects of light or nutrient on T_{opt} or θ. For example, in Bestion et al. (2018), the effect of nutrient limitation on θ was empirically parameterized as:

$$\theta = \theta_{min} + \frac{N}{N + K_N}(\theta_{max} - \theta_{min}) \tag{16}$$

where θ_{min} and θ_{max} represent θ values under totally nutrient deprivation and nutrient-replete conditions, respectively. However, one question of unifying Eq. 4 and Eq. 16 is how the interspecific relationship between μ_m and θ changes

with the availability of nutrients. Experimental data are needed to address this problem.

It is also possible that K_N can correlate with T_{opt}. Although current experimental evidences are insufficient to show (or dismiss) this pattern, a reasonable hypothesis is that warm-adapted species may require less nutrients than cold-adapted species (Toseland et al., 2013), leading to smaller values of K_N at high T_{opt}. If this were true, the temperature sensitivity of realized community growth rates under nutrient limitation will be greater than the estimations in this study. Again, more experimental data are needed to test this hypothesis.

While this study focuses on thermal traits, another important trait, cell size, also has significant effects on both the maximal growth rate (μ_m) and K_N (Litchman and Klausmeier, 2008; Ward et al., 2012; Marañón et al., 2013; Chen et al., 2019). In fact, together with optimal temperature, size has been used as a major trait axis of marine phytoplankton in the celebrated DARWIN model (Follows et al., 2007; Barton et al., 2010; Dutkiewicz et al., 2020). With multiple traits, it becomes more complicated to evaluate the effect of trait diversity (including thermal diversity) on community temperature sensitivity because we not only need to consider the variance of one trait, but also the covariance between traits (Savage et al., 2007; Le Gland et al., 2020). Using the second order Taylor expansion, the community growth rate under a given set of environmental condition can be expressed as a function of the mean and (co)variances of the traits:

$$\begin{aligned} \mu_w &= \iint \mu(l,\theta)\, dl\, d\theta \\ &\approx \mu(\bar{l},\bar{\theta}) + \Big[\frac{1}{2}\Big(\sigma_l^2 \frac{\partial^2 \mu}{\partial l^2} + \sigma_\theta^2 \frac{\partial^2 \mu}{\partial \theta^2}\Big) + \sigma_{l\theta} \frac{\partial^2 \mu}{\partial l \partial \theta}\Big]\Big|_{l=\bar{l},\theta=\bar{\theta}} \end{aligned} \tag{17}$$

in which l is log size and σ_l^2 is the variance of log size quantifying the size diversity. $\sigma_{l\theta}$ is the covariance between log size and optimal temperature. Thus, to evaluate the temperature sensitivity of the community growth rate, we need to consider the effects of the three (co)variance terms on μ_w. This will be a

future direction to work on.

4.3. Interpreting experimental estimation of activation energy from natural assemblages

Substantial efforts have been made to estimate the temperature sensitivity of natural assemblages from field experiments (Agawin et al., 1998; Yvon-Durocher et al., 2010; Chen et al., 2012; Marañón et al., 2014; Regaudie-de Gioux and Duarte, 2012; Chen and Liu, 2015; Vaquer-Sunyer and Duarte, 2013; Liu et al., 2018). Most studies can be classified into two categories. The first is to run a single regression of growth rate or production against temperature for a pooled dataset in which all the data points were collected at different locations and times. These studies tend to yield an activation energy around 0.3 and 0.4 eV (Chen et al., 2012; Regaudie-de Gioux and Duarte, 2012) or even lower if nutrient limitation is taken into account (Marañón et al., 2014). The second type is to artificially set up a temperature gradient under which the production or growth rates of the phytoplankton community are measured (Chen and Liu, 2015; Vaquer-Sunyer and Duarte, 2013; Liu et al., 2018; Menden-Deuer et al., 2018). This type of studies are mostly restricted to coastal environments due to sampling convenience and may generate a higher activation energy than the first one. Based on the above theoretical analysis and numerical simulations, it can be seen that the true temperature sensitivity of the phytoplankton community (E_w) is not a static value and cannot be easily estimated from environmental temperature. Nonetheless, some approximations can be made. For example, across large temperature gradients, $\overline{T_{opt}}$ more or less tracks mean environmental temperature so that the activation energy computed from the first type of the studies would approach E_i. The estimation of activation energy would more approximate E_a if $\overline{T_{opt}} \gg T$ (Chen and Liu, 2015) and be smaller if T approaches $\overline{T_{opt}}$ (Liu et al., 2018). However, it must be noted that the calculation of E_w in the present study (Eq. 8) is based on the infinitesimal increase of temperature, while in practice, the experimental temperature setup has to span a minimal range such as 5 °C. Both the location and the range of experimental temper-

atures relative to $\overline{T_{opt}}$, which unfortunately is hard to predict beforehand, will have significant effects on the estimated E_w. This complexity might be part of the reason that experimental estimates of activation energy can be highly variable (Liu et al., 2018).

4.4. Implications for future experimental work

This study suggests that we need more observations of *in situ* thermal trait distributions, particularly for microbial organisms. While many studies use environment-species associations or species distribution models to estimate the species' preferred temperature from field data (Irwin et al., 2012; Stuart-Smith et al., 2017; Burrows et al., 2019), these estimated thermal traits are confounded by other correlative environmental factors and using these trait to infer how the community will respond to future warming suffers from reasoning circularity (de Bello et al., 2021). Some authors have found discrepancies between the traits estimated from lab experiments (i.e., fundamental niche) and from environment-species associations (i.e., realized niche) (Soberón and Arroyo-Peña, 2017; Smith et al., 2021). As such, it would be best if we can directly measure thermal traits *in situ* (de Bello et al., 2021).

However, it is not easy to estimate *in situ* T_{opt} of microbial organisms reliably due to their acclimative capacity. There are two different approaches to measure T_{opt} *in situ*. The first approach is to isolate single-cell clones and measure their T_{opt} in the lab (Anderson and Rynearson, 2020; Strock and Menden-Deuer, 2021). The advantages of this method are: 1) the traits can be measured at very fine levels of taxonomy (i.e., we can obtain intraspecific trait diversity); 2) the organisms can be fully acclimated to the desired environmental condition, thus avoiding short-term temperature shock. However, there are two problems associated with this method. The first is that there is no guarantee that the isolate strains can fully represent the community in the field. Some strains still cannot be cultured until now. The second problem is that the culture temperatures would inevitably differ from those in the field and hence the measured thermal traits may differ from those *in situ* due to phenotypic plasticity. The second

approach is to run field experiments to measure the growth or metabolic rates along a gradient of temperature immediately after water samples are taken, thus ensuring that the measured traits represent the target community. However, this approach also suffers from a number of problems including the possibility of "thermal shock" and the difficulty to measure traits at the individual or even the species level. Nonetheless, despite the above challenges, it is still worth the efforts to measure the thermal traits of the community members; it is better to have some information than nothing. It is likely that we may draw relatively robust inferences based on a combination of the two different approaches.

Acknowledgments

I thank David J. S. Montagnes for helpful discussion. This research was funded by the Hong Kong Branch of Southern Marine Science and Engineering Guangdong Laboratory (Guangzhou) (SMSEGL20SC02) and a Leverhulme Trust Research Project Grant (RPG-2020-389).

References

Agawin, N.S., Duarte, C.M., Agusti, S., 1998. Growth and abundance of synechococcus sp. in a mediterranean bay: seasonality and relationship with temperature. Marine Ecology Progress Series 170, 45–53.

Aksnes, D., Egge, J., 1991. A theoretical model for nutrient uptake in phytoplankton. Marine ecology progress series. Oldendorf 70, 65–72.

Anderson, S.I., Rynearson, T.A., 2020. Variability approaching the thermal limits can drive diatom community dynamics. Limnology and Oceanography 65, 1961–1973.

Angilletta Jr, M.J., Angilletta, M.J., 2009. Thermal adaptation: a theoretical and empirical synthesis. Oxford University Press.

Angilletta Jr, M.J., Huey, R.B., Frazier, M.R., 2009. Thermodynamic effects on organismal performance: is hotter better? Physiological and Biochemical Zoology 83, 197–206.

Barton, A.D., Dutkiewicz, S., Flierl, G., Bragg, J., Follows, M.J., 2010. Patterns of diversity in marine phytoplankton. Science 327, 1509–1511.

Barton, S., Yvon-Durocher, G., 2019. Quantifying the temperature dependence of growth rate in marine phytoplankton within and across species. Limnology and Oceanography 64, 2081–2091.

de Bello, F., Carmona, C.P., Dias, A.T., Götzenberger, L., Moretti, M., Berg, M.P., 2021. Handbook of trait-based ecology: from theory to R tools. Cambridge University Press.

Bestion, E., Schaum, C.E., Yvon-Durocher, G., 2018. Nutrient limitation constrains thermal tolerance in freshwater phytoplankton. Limnology and Oceanography Letters 3, 436–443.

Boersma, M., Grüner, N., Signorelli, N.T., González, P.E.M., Peck, M.A., Wiltshire, K.H., 2016. Projecting effects of climate change on marine systems: is the mean all that matters? Proc. R. Soc. B 283, 20152274.

Brown, J.H., Gillooly, J.F., Allen, A.P., Savage, V.M., West, G.B., 2004. Toward a metabolic theory of ecology. Ecology 85, 1771–1789.

Burrows, M.T., Bates, A.E., Costello, M.J., Edwards, M., Edgar, G.J., Fox, C.J., Halpern, B.S., Hiddink, J.G., Pinsky, M.L., Batt, R.D., et al., 2019. Ocean community warming responses explained by thermal affinities and temperature gradients. Nature Climate Change 9, 959–963.

Chen, B., 2015. Patterns of thermal limits of phytoplankton. Journal of Plankton Research 37, 285–292.

Chen, B., Landry, M.R., Huang, B., Liu, H., 2012. Does warming enhance the effect of microzooplankton grazing on marine phytoplankton in the ocean? Limnology and oceanography 57, 519–526.

Chen, B., Laws, E.A., 2017. Is there a difference of temperature sensitivity between marine phytoplankton and heterotrophs? Limnology and Oceanography 62, 806–817.

Chen, B., Liu, K., 2015. Responses of autotrophic and heterotrophic rates of plankton from a subtropical coastal site to short-term temperature modulations. Marine Ecology Progress Series 527, 59–71.

Chen, B., Smith, S.L., Wirtz, K.W., 2019. Effect of phytoplankton size diversity on primary productivity in the north pacific: trait distributions under environmental variability. Ecology letters 22, 56–66.

Clarke, A., 2004. Is there a universal temperature dependence of metabolism? Functional Ecology 18, 252–256.

Dell, A.I., Pawar, S., Savage, V.M., 2011. Systematic variation in the temperature dependence of physiological and ecological traits. Proceedings of the National Academy of Sciences 108, 10591–10596.

Dutkiewicz, S., Cermeno, P., Jahn, O., Follows, M.J., Hickman, A.E., Taniguchi, D.A., Ward, B.A., 2020. Dimensions of marine phytoplankton diversity. Biogeosciences 17, 609–634.

Edwards, K.F., Thomas, M.K., Klausmeier, C.A., Litchman, E., 2016. Phytoplankton growth and the interaction of light and temperature: A synthesis at the species and community level. Limnology and Oceanography 61, 1232–1244.

Eppley, R.W., 1972. Temperature and phytoplankton growth in the sea. Fish. bull 70, 1063–1085.

Field, C.B., Behrenfeld, M.J., Randerson, J.T., Falkowski, P., 1998. Primary production of the biosphere: integrating terrestrial and oceanic components. science 281, 237–240.

Follows, M.J., Dutkiewicz, S., Grant, S., Chisholm, S.W., 2007. Emergent biogeography of microbial communities in a model ocean. science 315, 1843–1846.

Regaudie-de Gioux, A., Duarte, C.M., 2012. Temperature dependence of planktonic metabolism in the ocean. Global Biogeochemical Cycles 26.

Huey, R.B., Deutsch, C.A., Tewksbury, J.J., Vitt, L.J., Hertz, P.E., Pérez, H.J.Á., Garland, T., 2009. Why tropical forest lizards are vulnerable to climate warming. Proceedings of the Royal Society of London B: Biological Sciences 276, 1939–1948.

Huey, R.B., Kingsolver, J.G., 1989. Evolution of thermal sensitivity of ectotherm performance. Trends in Ecology & Evolution 4, 131–135.

Huston, M., 1979. A general hypothesis of species diversity. The American Naturalist 113, 81–101.

Irwin, A.J., Nelles, A.M., Finkel, Z.V., 2012. Phytoplankton niches estimated from field data. Limnology and Oceanography 57, 787–797.

Johnson, F.H., Lewin, I., 1946. The growth rate of e. coli in relation to temperature, quinine and coenzyme. Journal of Cellular and Comparative Physiology 28, 47–75.

Knies, J.L., Kingsolver, J.G., Burch, C.L., 2009. Hotter is better and broader: thermal sensitivity of fitness in a population of bacteriophages. The American Naturalist 173, 419–430.

Kontopoulos, D.G., van Sebille, E., Lange, M., Yvon-Durocher, G., Barraclough, T.G., Pawar, S., 2020. Phytoplankton thermal responses adapt in the absence of hard thermodynamic constraints. Evolution 74, 775–790.

Kremer, C.T., Thomas, M.K., Litchman, E., 2017. Temperature-and size-scaling of phytoplankton population growth rates: Reconciling the eppley curve and the metabolic theory of ecology. Limnology and Oceanography 62, 1658–1670.

Kwiatkowski, L., Bopp, L., Aumont, O., Ciais, P., Cox, P.M., Laufkötter, C., Li, Y., Séférian, R., 2017. Emergent constraints on projections of declining primary production in the tropical oceans. Nature Climate Change 7, 355–358.

Le Gland, G., Vallina, S.M., Smith, S.L., Cermeño, P., 2020. Spead 1.0–a model for simulating plankton evolution with adaptive dynamics in a two-trait continuous fitness landscape applied to the sargasso sea. Geoscientific Model Development Discussions 2020, 1–54.

Litchman, E., Klausmeier, C.A., 2008. Trait-based community ecology of phytoplankton. Annual review of ecology, evolution, and systematics 39, 615–639.

Liu, K., Chen, B., Zhang, S., Sato, M., Shi, Z., Liu, H., 2018. Marine phytoplankton in subtropical coastal waters showing lower thermal sensitivity than microzooplankton. Limnology and Oceanography .

López-Urrutia, Á., San Martin, E., Harris, R.P., Irigoien, X., 2006. Scaling the metabolic balance of the oceans. Proceedings of the National Academy of Sciences 103, 8739–8744.

Marañón, E., Cermeño, P., Huete-Ortega, M., López-Sandoval, D.C., Mouriño-Carballido, B., Rodríguez-Ramos, T., 2014. Resource supply overrides temperature as a controlling factor of marine phytoplankton growth. PloS one 9, e99312.

Marañón, E., Cermeño, P., López-Sandoval, D.C., Rodríguez-Ramos, T., Sobrino, C., Huete-Ortega, M., Blanco, J.M., Rodríguez, J., 2013. Unimodal size scaling of phytoplankton growth and the size dependence of nutrient uptake and use. Ecology letters 16, 371–379.

McGill, B.J., Enquist, B.J., Weiher, E., Westoby, M., 2006. Rebuilding community ecology from functional traits. Trends in ecology & evolution 21, 178–185.

Menden-Deuer, S., Lawrence, C., Franzè, G., 2018. Herbivorous protist growth and grazing rates at in situ and artificially elevated temperatures during an arctic phytoplankton spring bloom. PeerJ 6, e5264.

Moisan, J.R., Moisan, T.A., Abbott, M.R., 2002. Modelling the effect of temperature on the maximum growth rates of phytoplankton populations. Ecological Modelling 153, 197–215.

Montagnes, D.J., Kimmance, S.A., Atkinson, D., 2003. Using q10: Can growth rates increase linearly with temperature? Aquatic Microbial Ecology 32, 307–313.

Norberg, J., 2004. Biodiversity and ecosystem functioning: a complex adaptive systems approach. Limnology and Oceanography 49, 1269–1277.

Ohman, M., Hirche, H.J., 2001. Density-dependent mortality in an oceanic copepod population. Nature 412, 638–641.

Pawar, S., Dell, A.I., Savage, V.M., Knies, J.L., 2016. Real versus artificial variation in the thermal sensitivity of biological traits. The American Naturalist 187, E41–E52.

R Core Team, 2021. R: A Language and Environment for Statistical Computing. R Foundation for Statistical Computing. Vienna, Austria. URL: `https://www.R-project.org/`.

Sarmiento, J.L., Slater, R., Barber, R., Bopp, L., Doney, S.C., Hirst, A., Kleypas, J., Matear, R., Mikolajewicz, U., Monfray, P., et al., 2004. Response of ocean ecosystems to climate warming. Global Biogeochemical Cycles 18.

Savage, V.M., Webb, C.T., Norberg, J., 2007. A general multi-trait-based framework for studying the effects of biodiversity on ecosystem functioning. Journal of theoretical biology 247, 213–229.

Sherman, E., Moore, J.K., Primeau, F., Tanouye, D., 2016. Temperature influence on phytoplankton community growth rates. Global Biogeochemical Cycles 30, 550–559.

Smith, A.N., Hennon, G.M., Zinser, E.R., Calfee, B.C., Chandler, J.W., Barton, A.D., 2021. Comparing prochlorococcus temperature niches in the lab and across ocean basins. Limnology and Oceanography .

Smith, D.J., Amarasekare, P., 2018. Toward a mechanistic understanding of thermal niche partitioning. The American Naturalist 191, E57–E75.

Smith, S.L., 2011. Consistently modeling the combined effects of temperature and concentration on nitrate uptake in the ocean. Journal of Geophysical Research: Biogeosciences 116.

Smith, T.P., Thomas, T.J., García-Carreras, B., Sal, S., Yvon-Durocher, G., Bell, T., Pawar, S., 2019. Community-level respiration of prokaryotic microbes may rise with global warming. Nature communications 10, 1–11.

Soberón, J., Arroyo-Peña, B., 2017. Are fundamental niches larger than the realized? testing a 50-year-old prediction by hutchinson. PLoS One 12, e0175138.

Strock, J.P., Menden-Deuer, S., 2021. Temperature acclimation alters phytoplankton growth and production rates. Limnology and Oceanography 66, 740–752.

Stuart-Smith, R.D., Edgar, G.J., Bates, A.E., 2017. Thermal limits to the geographic distributions of shallow-water marine species. Nature Ecology & Evolution 1, 1846–1852.

Taucher, J., Oschlies, A., 2011. Can we predict the direction of marine primary production change under global warming? Geophysical Research Letters 38.

Thingstad, T.F., Aksnes, D.L., 2019. Why growth of nutrient-limited microorganisms should have low-temperature sensitivity. The ISME journal 13, 557–558.

Thomas, M.K., Aranguren-Gassis, M., Kremer, C.T., Gould, M.R., Anderson, K., Klausmeier, C.A., Litchman, E., 2017. Temperature–nutrient interactions

exacerbate sensitivity to warming in phytoplankton. Global change biology 23, 3269–3280.

Thomas, M.K., Kremer, C.T., Klausmeier, C.A., Litchman, E., 2012. A global pattern of thermal adaptation in marine phytoplankton. Science 338, 1085–1088.

Toseland, A., Daines, S.J., Clark, J.R., Kirkham, A., Strauss, J., Uhlig, C., Lenton, T.M., Valentin, K., Pearson, G.A., Moulton, V., et al., 2013. The impact of temperature on marine phytoplankton resource allocation and metabolism. Nature Climate Change 3, 979.

Vallina, S.M., Ward, B., Dutkiewicz, S., Follows, M., 2014. Maximal feeding with active prey-switching: A kill-the-winner functional response and its effect on global diversity and biogeography. Progress in Oceanography 120, 93–109.

Vaquer-Sunyer, R., Duarte, C.M., 2013. Experimental evaluation of the response of coastal mediterranean planktonic and benthic metabolism to warming. Estuaries and coasts 36, 697–707.

Violle, C., Navas, M.L., Vile, D., Kazakou, E., Fortunel, C., Hummel, I., Garnier, E., 2007. Let the concept of trait be functional! Oikos 116, 882–892.

Ward, B.A., Dutkiewicz, S., Jahn, O., Follows, M.J., 2012. A size-structured food-web model for the global ocean. Limnology and Oceanography 57, 1877–1891.

Yvon-Durocher, G., Jones, J.I., Trimmer, M., Woodward, G., Montoya, J.M., 2010. Warming alters the metabolic balance of ecosystems. Philosophical Transactions of the Royal Society of London B: Biological Sciences 365, 2117–2126.